PLoS One. 2016; 11(2): e0148962. PMCID: PMC4747524
Published online 2016 Feb 9. doi: 10.1371/journal.pone.0148962

Voltage-Induced Ca^{2+} Release in Postganglionic Sympathetic Neurons in Adult Mice

Hong-Li Sun,[1,2] Wen-Chin Tsai,[3,4] Bai-Yan Li,[5] Wen Tao,[1] Peng-Sheng Chen,[3] and Michael Rubart[1,*]

Agustín Guerrero-Hernandez, Editor

[1]Riley Heart Research Center, Herman B. Wells Center for Pediatric Research, Indiana University School of Medicine, Indianapolis, Indiana, United States of America
[2]Department of Pharmacology, Harbin Medical University-Daqing, Daqing, Heilongjiang, China
[3]The Krannert Institute of Cardiology and Division of Cardiology, Department of Medicine, Indiana University School of Medicine, Indianapolis, Indiana, United States of America
[4]Division of Cardiology, Department of Medicine, Hualein Tzu-Chi General Hospital, Hualein, Taiwan
[5]Department of Biomedical Engineering, Indiana University–Purdue University at Indianapolis, Indianapolis, Indiana, United States of America
Cinvestav-IPN, MEXICO

Competing Interests: The authors have declared that no competing interests exist.

Conceived and designed the experiments: MR. Performed the experiments: HS WT BL WT PC MR. Analyzed the data: HS WT MR. Wrote the paper: MR.

* E-mail: mrubartv@iu.edu

Received 2014 Dec 24; Accepted 2016 Jan 26.

Abstract

Go to:

Recent studies have provided evidence that depolarization in the absence of extracellular Ca^{2+} can trigger Ca^{2+} release from internal stores in a variety of neuron subtypes. Here we examine whether postganglionic sympathetic neurons are able to mobilize Ca^{2+} from intracellular stores in response to depolarization, independent of Ca^{2+} influx. We measured changes in cytosolic $\Delta F/F_0$ in individual fluo-4 –loaded sympathetic ganglion neurons in response to maintained K^+ depolarization in the presence (2 mM) and absence of extracellular Ca^{2+} ($[Ca^{2+}]_e$). Progressive elevations in extracellular $[K^+]_e$ caused increasing membrane depolarizations that were of similar magnitude in 0 and 2 mM $[Ca^{2+}]_e$. Peak amplitude of $\Delta F/F_0$ transients in 2 mM $[Ca^{2+}]_e$ increased in a linear fashion as the membrane become more depolarized. Peak elevations of $\Delta F/F_0$ in 0 mM $[Ca^{2+}]_e$ were ~5–10% of those evoked at the same membrane potential in 2 mM $[Ca^{2+}]_e$ and exhibited an inverse U-shaped dependence on voltage. Both the rise and decay of $\Delta F/F_0$ transients in 0 mM $[Ca^{2+}]_e$ were slower than those of $\Delta F/F_0$ transients evoked in 2 mM $[Ca^{2+}]_e$. Rises in $\Delta F/F_0$ evoked by high $[K^+]_e$ in the absence of extracellular Ca^{2+} were blocked by thapsigargin, an inhibitor of endoplasmic reticulum Ca^{2+} ATPase, or the inositol 1,4,5-triphosphate (IP_3) receptor antagonists 2-aminoethoxydiphenyl borate and xestospongin C, but not by extracellular Cd^{2+}, the dihydropyridine antagonist nifedipine, or by ryanodine at concentrations that caused depletion of ryanodine-sensitive Ca^{2+} stores. These results support the notion that postganglionic

sympathetic neurons possess the ability to release Ca^{2+} from IP_3-sensitive internal stores in response to membrane depolarization, independent of Ca^{2+} influx.

Introduction

Go to:

Calcium ions play an important role in regulating a variety of neuronal processes, including excitability, gene transcription, synaptic plasticity, growth cone behavior, synaptogenesis, and neurotransmitter release [1,2]. Neurons use both extracellular and intracellular sources of calcium. Whereas voltage-gated calcium channels and receptor-operated channels such as the NMDA receptors enable Ca^{2+} influx from the extracellular space, inositol 1,4,5-trisphosphate (IP_3) receptors and ryanodine receptors distributed throughout the endoplasmic reticulum membrane are responsible for releasing Ca^{2+} from its internal stores [1]. The mechanism for triggering Ca^{2+} discharge from internal stores is unknown in some cases, and it is often assumed that Ca^{2+}-induced Ca^{2+} release secondary to Ca^{2+} entry is the prevailing mechanism underlying Ca^{2+} mobilization. More recent studies, however, provide evidence for the existence of a Ca^{2+} influx-independent, voltage-induced Ca^{2+} release mechanism in neurons. A skeletal muscle excitation-contraction coupling–like mechanism, wherein conformational changes of the dihydropyridine receptor directly gate the ryanodine receptor, has been reported for hippocampal neurons [3], hypothalamic magnocellular neurons [4], and ischemically injured spinal cord white matter [5]. On the other hand, voltage-induced, Ca^{2+} influx-independent, Ca^{2+} release form IP_3-sensitive stores has been reported for insect dorsal unpaired median neurons [6]. Overall, these studies suggest the possibility that voltage-induced Ca^{2+} release from internal stores may be a more general phenomenon in neurons than previously thought.

Sympathetic ganglion neurons have been demonstrated to express both dihydropyridine-sensitive L-type calcium channels [7–10] and ryanodine receptors [11,12], suggesting the possibility that a skeletal muscle-like, voltage-induced Ca^{2+} release occurs in these cells. Here, we tested the hypothesis that sympathetic ganglion neurons in adult mice possess the ability to mobilize Ca^{2+} from internal stores in response to membrane depolarization, independent of Ca^{2+} influx. Our results provide, to the best of our knowledge, the first evidence that postganglionic sympathetic neurons are capable of releasing Ca^{2+} from internal stores in response to prolonged depolarization in the absence of extracellular calcium. Surprisingly, however, this process does not require dihydropyridine or ryanodine receptors. Rather, depolarization causes Ca^{2+} release from IP_3-sensitive internal stores, utilizing a yet to be identified plasmalemmal voltage sensor. This process may constitute a novel mechanism coupling electrical activity to a rise in intracellular Ca^{2+} in sympathetic neurons.

Materials and Methods

Go to:

Preparation of sympathetic neurons

Sympathetic neurons were prepared in a manner previously described [13]. DBA/J mice at 2 to 3 months of age were sacrificed by cervical dislocation. The superior and stellate ganglia were removed under stereomicroscopy and immediately placed in chilled (4–8°C) sympathetic complete medium [DME-F12 medium supplemented with sodium bicarbonate, HEPES, penicillin/streptomycin, 5% fetal bovine serum, and $MITO^+$ Serum extender (Collaborative Res, Bedford, MA, USA)]. The ganglia were then incubated for 20 min at 37°C in a Earle's Balanced Salt solution (Sigma, St. Louis, MO, USA) containing 10 U/ml papain (Worthington Biochemical Corp., Lakewood, NJ, USA), followed by a 30-min incubation in Earle's Balanced Salt solution supplemented with 1.3 mg/ml type II collagenase (Worthington) and 2.2 mg/ml dispase II (Roche, Indianapolis, IN, USA). Cells were then dissociated by trituration with a fire-polished glass Pasteur pipette in trituration solution (sympathetic complete medium containing 1.8 mg/ml bovine serum albumin) and plated on poly-D-lysine–coated No.1 circular glass cover slips. The isolated neurons were maintained in 5% CO_2-95% O_2 at 37°C in trituration solution and used ~24 hours after plating. All procedures were approved by the Indiana University

School of Medicine Institutional Animal Care and Use Committee.

Cytosolic Ca^{2+} imaging

A coverslip containing sympathetic neurons was transferred to a 263-µl recording chamber (model RC-21BRFS, Warner Instruments, Hamden, CT). Cells were loaded at room temperature with fluo-4 by incubation with the acetoxymethyl (AM) ester form of the dye (fluo-4/AM; Life Technologies, Grand Island, NY) at a final concentration of 2 µM in normal Tyrode's solution. After 20 min, cells were washed several times with dye-free Tyrode's solution and transferred to an inverted microscope (Axioscope) equipped with a Zeiss x63 1.4 numerical aperture water immersion lens. The microscope was attached to a confocal laser-scanning unit (Zeiss LSM 510). Fluo-4 fluorescence was probed every second by illumination with 488-nm laser light and emission was detected between 500 and 550 nm. The diameter of the pinhole was set to its maximum for all measurements. Images were taken in frame-mode at a pixel density of 512 x 512. Fluorescence signals were digitized at 8-bit resolution and analyzed using Metamorph software (Molecular Probes, Sunnyvale, CA). To quantitate amplitude and time course of changes in cytosolic fluo-4 fluorescence, i.e., Ca^{2+}, signal intensities of pixels located inside the neuron soma (excluding the nuclei) were measured, spatially averaged, and background corrected [F(t)]. Background fluorescence was measured as the average of a 40 x 40 pixel cell-free area outside the neuron soma of interest in each frame of every time series. Baseline fluorescence intensity (F_0) was determined by averaging F over the 10-s interval preceding the cell's exposure to elevated $[K^+]$ in the extracellular medium ($[K^+]_e$), and the time course of normalized fractional dye fluorescence [$\Delta F/F_0(t)$] was obtained, where ΔF equals $F(t)- F_0$. Signal correction for bleaching was not necessary.

Cells were exposed to a high $[K^+]$ solution (40, 60, 80 or 100 mM KCl) in the presence of 2 mM Ca^{2+} for 30 s, followed by a 1-min exposure to normal Tyrode's solution. A second 30-s exposure to the same $[K^+]_e$ in the absence of extracellular Ca^{2+} (with 200 µM EGTA added to the extracellular solution) was applied, and then the high $[K^+]_e$ solution was replaced with Ca^{2+}-free normal Tyrode's solution. The first and second applications of high $[K^+]_e$ were separated by 3-min exposures to Ca^{2+}-free normal Tyrode's solution. Bath solution exchanges were performed via manual injections (~500 µl/s) through the input port of the perfusion chamber. For each consecutive bath fluid exchange in the experimental protocol, the injected volume was 7 ml, corresponding to ~27 times the chamber volume. Solution changes were rapid, based on the fast and steady change in membrane potential achieved when cells were exposed to external solutions with elevated $[K^+]$ (see Fig 1C). Nominally Ca^{2+}-free Tyrode's solution contained the following (in mM): 140 NaCl, 5 KCl, 1 $MgCl_2$, 0.2 EGTA, 10 HEPES, and 10 D-glucose (pH 7.4). Assuming a 50 µM total contaminating Ca^{2+}, the free $[Ca^{2+}]_e$ was estimated to be ~ 43 nM [14,15]. For Ca^{2+}-containing Tyrode's solution, calcium was added (2 mM) and EGTA was omitted. When stimulating with elevated $[K^+]_e$, Na^+ was adjusted to maintain osmolarity [10,16]. Where indicated, drugs were added 20 min before and included throughout the stimulation. Pilot experiments demonstrated that the magnitude of the high $[K^+]_e$-elicited Ca^{2+} response in Ca^{2+}-free bath solution gradually decreased with consecutive $[K^+]_e$ tests. Therefore, the response to one tandem only of high $[K^+]_e$ exposure (in 2 and 0 mM $[Ca^{2+}]_e$) was tested in an individual neuron.

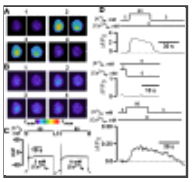

Fig 1

High $[K^+]_e$-induced intracellular Ca^{2+} transients in the presence and absence of extracellular Ca^{2+}.

Electrophysiology

Whole-cell voltage- and current-clamp recordings were performed at room temperature using a Multiclamp 700B

patch-clamp amplifier (Molecular Devices, Sunnyvale, CA, USA). Patch pipettes were pulled in a model P-97 puller (Sutter Instruments, Novato, CA, USA) from borosilicate glass capillaries and heat-polished prior to use with a Narishige MF-83 microforge (Narishige Inc., East Meadow, NY, USA). When filled with internal solution, the pipette resistance ranged from 2 to 5 MΩ. During the recording, changes in the bath solution were made by gravity driven perfusion. Pipette capacitance was zeroed on sealing. Whole-cell capacitive transients were compensated by 60–80%. Residual linear capacitive and leak currents were subtracted by the–*P*/6 method. Currents and voltages were low-pass filtered at 1 kHz and 5 kHz, respectively, using the built-in four-pole Bessel filter and sampled at 5 and 25 kHz, using a Digidata 1440A, acquired using Clampex10 and analyzed with Clampfit10 (all from Molecular Devices). Data collection was started ~2 to 3 min following membrane breakthrough.

Pipette solution for measuring whole-cell Ca^{2+} currents contained (in mM) 120 Cs-Aspartate, 1 $MgCl_2$, 4 MgATP, 0.3 Na_2GTP, 10 EGTA and 10 HEPES (pH 7.2), whereas the bath solution was composed of (in mM) 140 TEA-Cl, 2 $MgCl_2$, 2 $CaCl_2$, 10 glucose and 10 HEPES (pH 7.4). For measuring ion currents through voltage-gate Ca^{2+} channels in the absence of extracellular Ca^{2+}, the bath solution contained (in mM) 140 NaCl, 2 $MgCl_2$, 0.2 EGTA, 10 glucose and 10 HEPES (pH 7.4). For measuring action potentials, the pipette solution contained (in mM) 145 K-Aspartate, 2 $MgCl_2$, 5 HEPES, 5 Na_2ATP and 1.1 EGTA (pH 7.2), and the bath solution consisted of (in mM) 140 NaCl, 5 KCl, 1 $MgCl_2$, 2 $CaCl_2$, 10 HEPES and 10 glucose (pH 7.4). For Ca^{2+}-free bath solutions, calcium was omitted and EGTA (0.2 mM) was added. When recording the effects of elevating $[K^+]_e$ on membrane potential, $[Na^+]$ was lowered to maintain osmolarity. Osmolarities of all bath and pipette solutions were adjusted to 310 and 315 mOsm, respectively, using mannitol. Membrane potentials were adjusted for liquid junction potentials unless stated otherwise.

To characterize voltage dependence of peak I_{Ca} and to determine the $I_{Ca.}$ activation curve, currents were evoked by 300-ms pulses ranging from -90 to +60 mV in steps of 5 mV. The interval between voltage steps was 10 s. The peak $I_{Ca.L}$ density at each potential was plotted as a function of test voltage to generate the *I-V* curves. Activation curves were fitted with the following Boltzmann distribution equation: $G/G_{max} = 1/\{1+\exp[V_{1/2} –V)/k]\}$, where G is the voltage-dependent calcium conductance, G_{max} is the maximal calcium conductance, $V_{1/2}$ is the potential at which activation is half-maximal, V is the membrane potential, and k is the slope. G values were determined by the following equation: $G = I_{max}/(V\text{-}E_{Ca})$, where E_{Ca} is the reversal potential.

To examine steady-state inactivation, the voltage that gave maximal peak current was used for subsequent protocols. Cells were administered a series of prepulses (-90 to 40 mV) lasting 300 ms, from a holding potential of -90 mV, followed, after a 20-ms gap at -90 mV, by a 300-ms depolarization to a voltage eliciting the maximal peak current (0 mV). The interval between conditioning prepulses was 10 s. The resulting curves were normalized and fitted using the following Boltzmann distribution equation: $I/I_{max} = 1/\{1 + \exp[(V–V_{1/2})/k]\} + C$, where I_{max} is the peak current elicited after the most hyperpolarized prepulse, V is the preconditioning pulse potential, and C is a constant.

The membrane capacitance was calculated from 5-mV hyperpolarizing and depolarizing steps (20 ms) applied from a folding potential of -70 mV according to the equation: $C_M = \tau/\Delta V * I_0/(1 –I_\infty/I_0)$, where C_M is membrane capacitance, τ is the time constant of the capacitance current relaxation, I_0 is the peak capacitive current determined by single exponential fit and extrapolation to the first sample point after the voltage step ΔV, and I_∞ is the amplitude of the steady-state current during the voltage step [17]. Capacitive currents were sampled at 25 kHz and filtered at 5 kHz.

Data analysis

Summarized data are expressed as means ± SEM. Statistical analyses were determined by paired *t*-test, unpaired

t-test, and parametric and non-parametric one-way analyses of variance coupled with the appropriate *post hoc* analyses to determine significance ($P < 0.05$). Fisher Exact test was used to determine differences of proportions.

Chemicals

Stock solutions of 2-aminoethoxydiphenyl borate (2-APB), nifedipine, ryanodine and thapsigargin were prepared in DMSO. The final DMSO concentration in the experimental solution did not exceed 1 μl/ml. Caffeine stock solution was prepared in ddH_2O. Stock solution of tetrakis (2-pyridylmethyl) ethylendiamine (TPEN) was prepared in ethanol, and xestospongin C stock solution was made in PBS.

Results

Go to:

High $[K^+]_e$-induced membrane depolarization evokes Ca^{2+} transients in mouse sympathetic ganglion neurons in the absence of extracellular Ca^{2+}

Raising extracellular $[K^+]$ has been previously shown by others to produce stable and reproducible membrane depolarization in sympathetic ganglion neurons in culture, increasing intracellular free $[Ca^{2+}]$ in the presence of external Ca^{2+} [10]. Here, we combined $[K^+]_e$ depolarization with fluorescent Ca^{2+} imaging to examine the possibility that membrane depolarization evokes Ca^{2+} transients within isolated sympathetic ganglion neurons of adult mice not only in the presence of extracellular Ca^{2+} but also in its absence. Representative Ca^{2+} responses of two fluo-4/AM-loaded neurons elicited by consecutive 30-s exposures to 80 mM $[K^+]_e$ in the presence of 2 mM $[Ca^{2+}]_e$ and in Ca^{2+}-free bath solution (with 200 μM EGTA added) are illustrated in Fig 1A and 1B, respectively. Elevating $[K^+]_e$ in normal Ca^{2+} gave rise to increases in global fluorescence intensity, which were larger in the nuclei than in the cytosols (Fig 1A). The fluorescence signals remained elevated throughout the exposure to high $[K^+]_e$ (panels 2 and 3 in Fig 1A) and returned to baseline values following restoration of $[K^+]_e$ (panel 4 in Fig 1A). The $[K^+]_e$ challenge was repeated in the absence of extracellular Ca^{2+} following a 3-min exposure to Ca^{2+}-free normal Tyrode's solution. As illustrated in Fig 1B, a second 30-s exposure to 80 mM $[K^+]$ in the absence of external Ca^{2+} gave rise to sustained elevations in intracellular Ca^{2+} (panels 2 and 3 in Fig 1B), although the magnitude of the effect was markedly reduced compared to the 2 mM $[Ca^{2+}]_e$ condition. Fluorescence signal intensity recovered upon restoration of $[K^+]_e$ in the continued absence of extracellular Ca^{2+}.

To make certain that membrane depolarization evoked by 80 mM $[K^+]_e$ was maintained at similar potentials in the presence and absence of external Ca^{2+}, the membrane potential was recorded from isolated sympathetic neurons before and during the 30-s depolarization. A representative example is shown in Fig 1C. Both in the presence and absence of extracellular Ca^{2+}, high $[K^+]_e$ rapidly depolarized the neuron following the solution change, and remained stable while $[K^+]_e$ = 80 mM. The magnitude of depolarization appeared similar under both conditions. After $[K^+]_e$ was restored to 5 mM, membrane potential exhibited a transient afterhyperpolarization in 2 mM $[Ca^{2+}]_e$. On average, the degree of membrane depolarization evoked by 80 mM $[K^+]_e$ in 0 mM $[Ca^{2+}]_e$ was slightly less than that in 2 mM $[Ca^{2+}]_e$ (see Table 1).

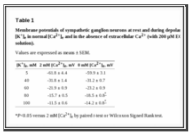

Table 1

Membrane potentials of sympathetic ganglion neurons at rest and during depolarization with elevated $[K^+]_e$ in normal $[Ca^{2+}]_e$ and in the absence of extracellular Ca^{2+} (with 200 μM EGTA added to the bath solution).

Next, we sought to quantitate the high $[K^+]_e$-evoked changes in cytosolic Ca^{2+} level, using $\Delta F/F_0$ as a measure. Plots of $\Delta F/F_0$ as a function of time for one of the neurons in Fig 1A and 1B are displayed in Fig 1D. The neuron

responds to high $[K^+]_e$ exposure with an initial peak followed by a slow, spontaneous decay, which was seen in all cells tested, despite the fact that the depolarization of the plasma membrane was maintained throughout the 30-s $[K^+]_e$ challenge. Increases in $\Delta F/F_0$ typically resolved within less than 15 s after restoration of $[K^+]_e$. Replacement of normal Tyrode's solution with Ca^{2+}-free solution did not evoke significant changes in cytosolic $[Ca^{2+}]$ (Fig 1D, middle panel), indicating that the solution change *per se* does not contribute to the rise in fluo-4 fluorescence seen in response to elevated $[K^+]_e$ in the absence of external Ca^{2+}. A 30-s exposure of the same neuron to 80 mM $[K^+]_e$ in Ca^{2+}-free bath solution evoked a low-amplitude Ca^{2+} transient which exhibited markedly slower rise and decay kinetics compared to the transient in 2 mM $[Ca^{2+}]_e$ (Fig 1D, lower panel). Overall, 47 (78%) of a total of 60 neurons responded with a rise in cytosolic $[Ca^{2+}]$ in the absence of extracellular Ca^{2+}. To assess whether loss of cellular viability gives rise to these marked differences in Ca^{2+} transient properties, a subset of neurons were re-exposed to high $[K^+]_e$ in normal $[Ca^{2+}]_e$ following the $[K^+]_e$ test in Ca^{2+} free conditions. A representative $\Delta F/F_0$ (t) tracing is shown in Fig 2A. After raising $[Ca^{2+}]_e$ to 2 mM, the peak amplitude of the high $[K^+]_e$-evoked Ca^{2+} transient clearly exceeded that of the preceding transient recorded in the absence of external Ca^{2+}, and its time course was indistinguishable from that of a response typically seen during initial exposures to high $[K^+]_e$ in 2 mM $[Ca^{2+}]_e$. Identical observations were made in 7 cells. These results prove that the neurons remain viable and support the notion that the differences in Ca^{2+} transient properties between 2 and 0 mM $[Ca^{2+}]_e$ are unlikely to result from unspecific effects of the exposure to the Ca^{2+} free bath solution. At 80 mM $[K^+]_e$, the average peak Ca^{2+} transient amplitude was markedly smaller in the absence than in the presence of external Ca^{2+} and their average rise and decay times were markedly prolonged compared to Ca^{2+} transients evoked in normal $[Ca^{2+}]_e$ (Fig 2B). Overall, these results suggest that a subpopulation of sympathetic neurons possess the ability to release Ca^{2+} from intracellular stores in response to prolonged membrane depolarization in the absence of extracellular Ca^{2+}.

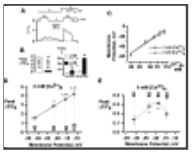

Fig 2

Sympathetic neurons possess the ability to release Ca^{2+} from intracellular stores in response to prolonged membrane depolarization in the absence of extracellular Ca^{2+}.

To relate the magnitude of the Ca^{2+} responses to membrane depolarization, we next recorded Ca^{2+} transients during exposure to various K^+ concentrations. In a parallel series of experiments, we measured membrane voltage in isolated neurons, using external solutions identical to those in the Ca^{2+} imaging experiments.

Exposure to 40, 60, 80 and 100 mM $[K^+]_e$ in 2 mM $[Ca^{2+}]_e$ caused progressively increasing membrane depolarizations (Table 1), yielding a slope of 67.5 mV per 10-fold change in $[K^+]_e$ (solid line in Fig 2C). Plotting the magnitude of peak $\Delta F/F_0$ transient amplitude against membrane potential (Fig 2D) revealed a linear increase over a range between -31.8 and -11.5 mV. Removal of Ca^{2+} from the extracellular solution did not significantly alter the resting membrane potential in 5 mM $[K^+]$ Tyrode's solution (Table 1). Progressive elevations in $[K^+]_e$ caused depolarizations that were of similar magnitude to those seen in 2 mM $[Ca^{2+}]_e$ (Table 1), giving rise to a slope of 62.2 mV per 10-fold change in $[K^+]_e$ (dashed line in Fig 2C). Over the voltage range examined (-31.2 to -14.2 mV), the magnitude of peak $\Delta F/F_0$ transient amplitude displayed an inverse U-shaped dependence on membrane potential as shown in Fig 2E, which is in sharp contrast to the linear rise in peak $\Delta F/F_0$ amplitude that was observed in response to progressively increasing membrane depolarizations in 2 mM $[Ca^{2+}]_e$ (Fig 2D).

The increase in the magnitude of Ca^{2+} transient amplitude with increasing depolarization in the presence of 2 mM extracellular Ca^{2+} suggested a role of voltage-gated Ca^{2+} channel activity in governing this relationship, as had been described previously in mammalian postganglionic sympathetic neurons [10,18]. Accordingly, to relate Ca^{2+} transient properties to Ca^{2+} channel activity, we measured whole-cell Ca^{2+} currents (I_{Ca}) over a wide range

of voltages including those generated by the lowest and highest $[K^+]_e$ used in the Ca^{2+} imaging experiments. Short depolarizations evoked Ca^{2+} currents exhibiting no, or very little, inactivation (Fig 3A). A plot of peak I_{Ca} as a function of voltage is shown in Fig 3B, exhibiting the typical bell-shaped dependence on membrane potential. The descending portion of the I_{Ca}-V curve largely coincided with the voltage range over which peak $\Delta F/F_0$ increased (see Fig 2D), suggesting that the membrane potential dependence of peak I_{Ca} controls Ca^{2+} transient magnitude over the range of membrane depolarizations studied here. This observation is in agreement with previous studies [10,18]. To examine whether depolarization-induced changes in Ca^{2+} channel gating underlie the membrane potential-dependence of peak $\Delta F/F_0$ in the absence of external Ca^{2+}, we next determined the voltage-dependence of Ca^{2+} channel activation. The result is shown in Fig 3C. The probability of the channel of being activated (P_{act}) increased in a sigmoidal fashion as the membrane potential became more depolarized. This behavior contrasts with the inverse U-shaped dependence of peak $\Delta F/F_0$ on voltage in Ca^{2+}-free bath solution (Fig 2E), suggesting that membrane potential-dependent changes in peak P_{act} of voltage-activated Ca^{2+} channels do not constitute the trigger for Ca^{2+} release in 0 mM $[Ca^{2+}]_e$.

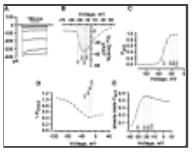

Fig 3

Peak magnitude of cytosolic $\Delta F/F_0$ transients as a function of calcium channel activity.

The slow kinetics of increase in $[Ca^{2+}]_i$ during sustained membrane depolarization in the absence of external Ca^{2+} (see Fig 2B) suggested the possibility that Ca^{2+} release is regulated by the steady-state activity of voltage-gated Ca^{2+} channels. The steady-state probability of a channel of being activated is the product of peak P_{act} (obtained from the activation curve in Fig 3C) and the probability of not being inactivated (1-P_{inact}), i. e., steady-state P_{act} = (peak P_{act}) * (1 –P_{inact}). Accordingly, we next determined the voltage-dependence of I_{Ca} inactivation. Channel inactivation displayed a U-shaped dependence on voltage (Fig 3D). Fits of the descending portion of the inactivation curve to a Boltzmann distribution revealed $V_{1/2}$ and k values of -55.3 mV and 16.3 mV, respectively. Fig 3E shows the relationship between membrane potential and steady-state P_{act}. Negative to -20 mV, steady-state P_{act} increased steeply, whereas it decreased slightly at less negative potentials. Thus, steady-state activation of voltage-gated Ca^{2+} channels and peak $\Delta F/F_0$ in the absence of external Ca^{2+} shared a similar, i.e., inverse U-shaped, dependence on membrane potential over identical voltage ranges, suggesting that magnitudes of changes in the depolarization-induced $[Ca^{2+}]_i$ in 0 mM $[Ca^{2+}]_e$ are controlled by the steady-state gating of voltage-activated Ca^{2+} channels.

Depolarization in Ca^{2+} free solution induces Ca^{2+} release from IP_3-, but not ryanodine-, sensitive internal stores

To investigate the role of Ca^{2+} release from internal stores in mediating depolarization-induced increases in cytosolic $[Ca^{2+}]$, we next assessed the effects of the Ca^{2+}-ATPase inhibitor thapsigargin (1 μM) on high $[K^+]_e$-evoked Ca^{2+} responses in isolated sympathetic neurons. Neurons were pre-incubated with thapsigargin for 20 min while being loaded with fluo-4/AM and then subjected to Ca^{2+} imaging in the continued presence of the inhibitor. Representative plots of $\Delta F/F_0$ as a function of time are shown in Fig 4. A 30-s exposure to 80 mM $[K^+]_e$ in the presence of extracellular Ca^{2+} caused an increase in cytosolic $[Ca^{2+}]$. A second 30-s exposure to 80 mM $[K^+]$ in the absence of external Ca^{2+} did not evoke a significant increase in intracellular $[Ca^{2+}]$. Overall, only 2 (10.5%) of 19 thapsigargin-treated neurons developed Ca^{2+} transients during exposure to elevated $[K^+]_e$ in the absence of extracellular Ca^{2+} compared to 47 (78%) of 60 non-treated cells ($P < 0.001$; Fig 4B). To make certain that membrane depolarization evoked by 80 mM $[K^+]_e$ was maintained at similar potentials among thapsigargin-treated and non-treated neurons in the study, we compared membrane potentials recorded from

isolated sympathetic neurons before and during high $[K^+]_e$-induced depolarizations in the presence of the drug with those recorded in its absence. We found no significant differences in resting membrane potential or potentials obtained during the 80-mM $[K^+]_e$ challenges either in normal Ca^{2+} or Ca^{2+}-free bath solutions ($P > 0.05$) among the two experimental groups (Table 2). Collectively, these results indicate that thapsigargin-induced abolition of high $[K^+]_e$-Ca^{2+} transients in 0 mM $[Ca^{2+}]_e$ does not result from a collapse of the membrane potential but rather supports the notion that depolarization elicits Ca^{2+} release from intracellular stores independently of Ca^{2+} influx.

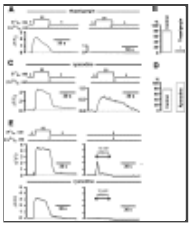

Fig 4

Thapsigargin, but not ryanodine, suppresses high $[K^+]_e$-induced cytosolic Ca^{2+} transients in the absence, but not in the presence, of extracellular Ca^{2+}.

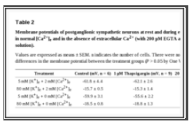

Table 2

Membrane potentials of postganglionic sympathetic neurons at rest and during exposure to 80 mM $[K^+]_e$ in normal $[Ca^{2+}]_e$ and in the absence of extracellular Ca^{2+} (with 200 μM EGTA added to the bath solution).

Depolarization-evoked cytosolic Ca^{2+} transients in the absence of extracellular Ca^{2+} could result from conformational coupling between L-type Ca^{2+} channels and ryanodine receptors, as in skeletal muscle excitation-contraction coupling [4,19]. Accordingly, we examined the effect of pharmacological blocking Ca^{2+} release from ryanodine-sensitive stores on depolarization-induced Ca^{2+} release. We found that pretreating neurons for 20 min with ryanodine (20 μM) spared the high $[K^+]_e$-induced Ca^{2+} responses both in the presence and absence of extracellular Ca^{2+} (Fig 4C). Overall, there was no significant difference in the proportion of neurons exhibiting $[K^+]$-induced Ca^{2+} elevations in 0 mM $[Ca^{2+}]_e$ between the ryanodine [14 (100%) of 14 cells] and the control group [47 (78%) of 60 cells; $P > 0.05$; Fig 4D]. As a probe for ryanodine receptor function, we applied caffeine (10 mM), an agonist of ryanodine receptor-mediated Ca^{2+} release, and monitored intracellular $[Ca^{2+}]$. Exposures to 80 mM $[K^+]_e$ and caffeine both reversibly elevated cytosolic $[Ca^{2+}]$. Pretreatment with 20 μM ryanodine abrogated the caffeine response, but did not affect the high $[K^+]_e$-induced response, which is consistent with previous studies (Fig 4E) [10], but differs from other studies demonstrating changes of $[Ca^{2+}]_i$ transient amplitude and/or kinetics by ryanodine [14,18]. Identical observations were made in 3 more cells. Thus, depolarization-evoked Ca^{2+} release in sympathetic ganglion neurons does not require ryanodine receptors, ruling out a skeletal muscle excitation-contraction coupling-like mechanism.

We then examined the contribution of Ca^{2+} release from IP_3-sensitive Ca^{2+} stores to depolarization-induced Ca^{2+} transients in the absence of external Ca^{2+}. Previous studies had demonstrated that depolarization of insect dorsal unpaired neurons in the absence of external Ca^{2+} triggers Ca^{2+} release from IP_3-sensitive stores [6]. To determine whether IP_3 receptors contribute to depolarization-evoked Ca^{2+} signaling in sympathetic ganglion neurons, we pharmacologically blocked release from IP_3-sensitive stores and then measured 80 mM $[K^+]_e$-induced changes in cytosolic $[Ca^{2+}]$. We found that pretreating the neurons for 20 min with the IP_3 receptor inhibitors 2-aminoethoxydiphenyl borate (2-APB; 20 μM) or xestospongin C (10 μM) abolished the $[K^+]_e$-evoked Ca^{2+} transient in the absence, but not in the presence, of extracellular Ca^{2+} (Fig 5A). Overall, exposure to elevated $[K^+]_e$ in 0 mM $[Ca^{2+}]_e$ induced Ca^{2+} transients in only 1 (17%) of 6 2-APB–treated and 2 (10.5%) of 16 xestospongin C- treated neurons, compared to 47 (78%) of 60 control neurons ($P = 0.001$; Fig 5B). The

prevalence of non-responding cells was similar following treatment with 2-APB or xestospongin C ($P > 0.05$). Further, we found no significant differences in resting membrane potential or potentials obtained during the 80-mM $[K^+]_e$ challenges either in normal $[Ca^{2+}]_e$ or Ca^{2+}-free bath solutions ($P > 0.05$) between control neurons and neurons following IP_3 receptor blockade (Table 2). Collectively, these results support the notion that membrane depolarization in the absence of extracellular Ca^{2+} triggers Ca^{2+} release from IP_3-sensitive internal stores, leading to slow rises in cytosolic $[Ca^{2+}]$.

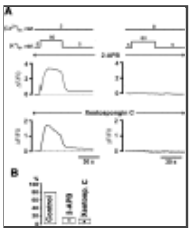

Fig 5

Pharmacological inhibitors of IP_3 receptors abrogate high $[K^+]_e$-induced Ca^{2+} transients in Ca^{2+}-free bath solution.

Depolarization-evoked Ca^{2+} release in the absence of extracellular Ca^{2+} does not require L-type Ca^{2+} channels

Voltage-dependent changes in L-type Ca^{2+} channel (dihydropyridine receptor) gating have previously been identified as the mechanism linking membrane depolarization to Ca^{2+} release from IP_3-sensitive stores in skeletal myotubes in the absence of extracellular Ca^{2+} [20]. If an identical mechanism is at work in sympathetic ganglion neurons, we would expect the 1,4-dihydropyridine L-type Ca^{2+} channel antagonist nifedipine, which acts on the channel by immobilizing its gating charge, to affect depolarization-evoked Ca^{2+} transients. Measurements of whole-cell currents through high voltage-activated Ca^{2+} channels (with Ba^{2+} as charge carrier) revealed that a high concentration of nifedipine (50 μM) was required to achieve a small (~-20%), yet significant, reduction in current amplitude (Fig 6A–6C). The finding that nifedipine at 10 μM did not block I_{Ba} strongly suggests a lack of functional L-type Ca^{2+} channels in adult sympathetic ganglion neurons, whereas the significant reduction of I_{Ba} at 50 μM nifedipine may reflect inhibition of $Ca_v2.x$ channels [21]. Alternatively, the insensitivity of whole-cell I_{Ba} to inhibition by nifedipine may suggest that adult sympathetic ganglion neurons express the skeletal muscle isoform of the L-type Ca^{2+} channel which has been shown previously to require nearly 50 μM nifedipine for complete block [22]. We found that pretreating neurons for 20 min with a high concentration of nifedipine (50 μM) spared the high $[K^+]_e$-induced Ca^{2+} responses both in the presence and absence of extracellular Ca^{2+} (Fig 6D). The lack of a significant effect of nifedipine on the magnitude of depolarization-evoked Ca^{2+} transients in the presence of normal $[Ca^{2+}]_e$ is consistent with the notion that Ca^{2+} entry via L-type Ca^{2+} channels does not contribute noticeably to the rise in global $[Ca^{2+}]$ in our study. Overall, there was no significant difference in the proportion of neurons exhibiting $[K^+]$-induced Ca^{2+} elevations in 0 mM $[Ca^{2+}]_e$ between the nifedipine [10 (100%) of 10 cells] and the control group [47 (78%) of 60 cells; $P > 0.05$; Fig 6E]. Collectively, these results support the notion that high $[K^+]_e$-evoked Ca^{2+} release in the absence of extracellular Ca^{2+} does not require L-type Ca^{2+} channels.

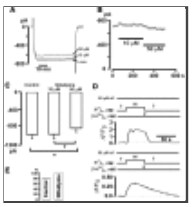

Fig 6

The 1,4-dihydropyridine antagonist of L-type Ca^{2+} channels, nifedipine, does not affect Ca^{2+} transients elicited by exposure to elevated $[K^+]_e$.

Depolarization-induced $[Ca^{2+}]_i$ transients in the absence of extracellular calcium are not blocked by extracellular cadmium

Voltage-gated calcium channels become permeable to monovalent cations when extracellular calcium concentrations fall to sub-micromolar levels [23], suggesting the possibility that depolarization–induced $[Ca^{2+}]_i$ increases in the absence of external Ca^{2+} are triggered by influx of Na^+ and/or K^+ through open calcium channels under our experimental conditions. Accordingly, we next examined the effect of pharmacologically inhibiting ion flux through high voltage-gated Ca^{2+} channels on $[K^+]_e$-Ca^{2+} transients in 0 mM $[Ca^{2+}]_e$. Extracellular Cd^{2+} has been shown previously to potently block ion flux through neuronal, high voltage-gated calcium channels in a concentration-dependent manner [10], without altering channel gating. Our measurements of whole-cell Ca^{2+} currents in voltage-clamped neurons (using Ba^{2+} as the charge carrier) confirmed the absence of resolvable inward currents following the addition of 300 μM Cd^{2+} to the bath solution (S1A–S1C Fig), supporting the notion that Cd^{2+} at this concentration potently blocked currents through voltage-activated Ca^{2+} channels, consistent with previous studies in adult sympathetic ganglion neurons [9,24]. In addition, Cd^{2+} at concentrations that block ion flux has been reported to not affect membrane potential of sympathetic ganglion neurons [10]. Thus, extracellular Cd^{2+} in micromolar concentrations should be ideally suited to distinguish a role of ion flux through versus gating of voltage-dependent Ca^{2+} channels in mediating depolarization-induced rise in $[Ca^{2+}]_i$ in 0 mM $[Ca^{2+}]_e$. A typical $\Delta F/F_0$ response of a sympathetic ganglion neuron to a 30-s exposure to 80 mM $[K^+]_e$ and 300 μM Cd^{2+} in the absence of external Ca^{2+} is shown in Fig 7A. In these conditions, high $[K^+]_e$ still caused an increase in $\Delta F/F_0$, with no sign of recovery following return to 5 mM $[K^+]_e$. The irreversible increase in fluo-4 fluorescence resulted from Cd^{2+} influx into the cell, because it was completely reversed by a 5-min incubation with the membrane-permeant divalent metal chelator tetrakis (2-pyridylmethyl) ethylendiamine (TPEN; 100 μM; Fig 7B), whose affinity for Cd^{2+} ($K_d = 10^{-12}$ M) [25] is several orders of magnitude higher than that for Ca^{2+} ($K_d = 10^{-4.4}$ M) [26]. The means of high $[K^+]_e$-induced changes in peak $\Delta F/F_0$ in the presence of 2 mM $[Ca^{2+}]_e$ were not significantly different before and after loading with TPEN (Fig 7C), suggesting that TPEN can be used to selectively suppress the Cd^{2+} influx-dependent component of the fluo-4 signal in our experimental conditions. Indeed, combined exposure of another TPEN-loaded neuron to 80 mM $[K^+]_e$ and 300 μM Cd^{2+} in the absence of external Ca^{2+} revealed the typical $\Delta F/F_0$ response pattern seen in the absence of Cd^{2+}, i.e., the increase in $\Delta F/F_0$ readily resolved following return to physiological $[K^+]_e$ (Fig 7D). Identical observations were made in 4 other TPEN-loaded neurons.

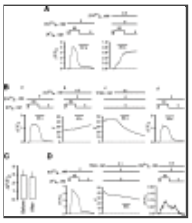

Fig 7

External Cd^{2+} does not suppress high $[K^+]_e$-induced $\Delta F/F_0$ transients in 0 mM $[Ca^{2+}]_e$.

To further examine whether voltage-dependent Ca^{2+} channels conduct Na^+ currents in the absence of extracellular Ca^{2+}, we sequentially measured macroscopic currents carried by these channels in 2 and 0 mM $[Ca^{2+}]_e$. Extracellular concentrations of Mg^{2+} (2 mM) and Na^+ (140 mM) remained unchanged. Tetrodotoxin (1 μM) was present in the bath solution throughout the measurements to block voltage-gated Na^+ channels. Exemplar whole-cell current traces acquired in response to step depolarizations to +10 mV before and after Ca^{2+} withdrawal are shown in Fig 8A. Removal of extracellular Ca^{2+} resulted in loss of inward currents, indicating that voltage-gated Ca^{2+} channels do not carry resolvable Na^+ currents in the ionic conditions used here. Overall, these results support the notion that depolarization-induced rises in $[Ca^{2+}]_i$ in 0 mM $[Ca^{2+}]_e$ are not triggered by ion fluxes through high voltage-gated Ca^{2+} channels.

Fig 8

Voltage-gated Ca^{2+} channels do not conduct Na^+ after removal of extracellular Ca^{2+}.

Our results indicate that the increase in global cytosolic [Ca^{2+}] seen in response to prolonged depolarization in nominally Ca^{2+}-free bath solution cannot be attributed to Ca^{2+} influx and subsequent Ca^{2+}-induced Ca^{2+} release. Further, a skeletal muscle excitation-contraction–like mechanism as reported previously for hypothalamic magnocellular neurons, ischemically injured spinal cord white matter, and hippocampal neurons, can be excluded as the mechanism underlying depolarization-induced Ca^{2+} mobilization [3–5]. On the other hand, our findings are similar to those reported previously by Ryglewski et al. demonstrating that insect dorsal unpaired median neurons are capable of transducing incremental depolarization into gradual increases in cytosolic [Ca^{2+}], involving Ca^{2+}- influx-independent activation of a G protein-phospholipase C-IP_3 receptor pathway. However, the nature of the voltage sensor was not identified in the latter study [6].

Na-induced dissociation of G-protein subunits has been demonstrated previously in neurons [27], suggesting the possibility that high $[K^+]_e$-evoked Ca^{2+} mobilization from IP_3-sensitive stores as seen in the present study involves an ion influx-dependent, but not strictly depolarization-dependent, mechanism. Specifically, Na^+ permeation of voltage-gated Ca^{2+} channels in the absence of external Ca^{2+} is one possible pathway linking Ca^{2+} release to membrane depolarization in our experimental conditions. We think this possibility to be unlikely for several reasons. First, extracellular Cd^{2+} at concentrations that completely blocked inward currents through voltage-gated Ca^{2+} channels, did not suppress high $[K^+]_e$-$[Ca^{2+}]_i$ transients in the absence of extracellular Ca^{2+}. Second, we did not detect resolvable inward currents through voltage-dependent Ca^{2+} channels in voltage-clamped, depolarized neurons upon removal of extracellular Ca^{2+}. Third, high $[K^+]_e$-Ca^{2+} transients in Ca^{2+}-free bath solutions could be readily evoked in the presence of 1 mM extracellular Mg^{2+}, which corresponds to 4 times the IC_{50} of Mg^{2+}-induced block of Na^+ current through N-type Ca^{2+} channels [28], the major subtype of voltage-gated Ca^{2+} channels in adult sympathetic ganglion neurons.

Also, ions other than Ca^{2+} can enter the cell via alternative voltage-modulated pathways, e.g., voltage-gated Na^+ channels, or voltage-independent pathways, e.g., acetylcholine receptor and/or transient receptor potential cation channels. The gradual decrease in Na^+ concentration in the bath solution for increasingly large depolarizations results in an incremental reduction in the Na^+ driving force, progressively reducing its flux through voltage-independent channels as the membrane becomes more depolarized. This behavior conflicts with the non-monotonic dependence of depolarization-evoked peak $\Delta F/F_0$ amplitude on voltage that we observed in the absence of external Ca^{2+} (see Fig 2E). It thus appears unlikely that the magnitude of Na^+ movement through voltage-independent pathways constitutes the trigger for Ca^{2+} mobilization in our experiments. Because the relationship between changes in membrane potential and those in extracellular K^+ concentration followed the Nernst equation with a slope close to that expected for a K^+-selective ion channel (see Fig 2C), the K^+ net flux at each membrane potential achieved with various $[K^+]_e$ must have been zero or close to zero, excluding voltage-dependent changes in transmembrane K^+ flux as a possible regulator of Ca^{2+} release in 0 mM $[Ca^{2+}]_e$.

Finally, the possibility that the voltage-dependence of peak $\Delta F/F_0$ magnitude in the absence of external Ca^{2+} reflects the voltage-dependence of a steady-state current through voltage-gated Na^+ channels has to be considered. Previous studies by others revealed the existence of a non-inactivating component of the Na^+ current in neurons [29], whose magnitude exhibits a non-monotonic, U-shaped, dependence on voltage. However, these persistent, so-called 'window' Na^+ currents activated at voltages significantly more negative than those of peak $\Delta F/F_0$ in 0 mM $[Ca^{2+}]_e$, making persistent Na^+ currents an unlikely candidate linking Ca^{2+} discharge to membrane voltage changes. Overall, our results thus support the notion that depolarization *per se* suffices to trigger Ca^{2+} discharge from IP_3-sensitive stores in 0 mM $[Ca^{2+}]_e$.

The inverse U-shaped dependence of peak $\Delta F/F_0$ amplitude on membrane potential in 0 mM $[Ca^{2+}]_e$ is both unexpected and puzzling. Because peak P_{act} of voltage-gated Ca^{2+} channels steeply increases with

depolarization over the range of membrane potentials we studied, we can exclude the possibility that gating changes as are typically achieved during peak activation of these channels, underlie voltage-induced, Ca^{2+} influx-independent Ca^{2+} release in our experiments. However, the observed non-monotonic behavior of Ca^{2+} signal strength with increasing depolarization is compatible with a mechanism, wherein the voltage-dependence of a channel's steady-state, but not peak, P_{act} serves to transduce prolonged changes in membrane potential into graded Ca^{2+} mobilization. Indeed, our numerical simulations using experimentally determined activation and inactivation properties of voltage-activated Ca^{2+} channels demonstrate that the channel's voltage-dependence of steady-state P_{act} on membrane potential overlaps with that of peak $\Delta F/F_0$ magnitude measured in 0 mM $[Ca^{2+}]_e$. Direct proof of the role of conformational changes of a Ca^{2+} channel complex in tuning Ca^{2+} discharge from IP_3-sensitive internal stores will require experimental immobilization of gating charges in subtypes of voltage-gated Ca^{2+} channels known to be expressed in adult sympathetic ganglion neurons, including N- and P/Q-type Ca^{2+} channels. It will also require measurements of absolute free $[Ca^{2+}]_i$ levels. Because we have not calibrated the fluo-4 signal for our experimental conditions, we were unable to directly correlate changes in membrane potential to those in free $[Ca^{2+}]_i$.

Besides voltage-gated ion channels, it is possible that non-ion channel proteins act as voltage sensors, e.g., the Na-K ATPase, the Na-Ca exchanger or the recently discovered voltage-sensitive phosphatide phosphatase, although expression of the latter in mammalian neuronal tissue has not yet been confirmed [30]. Additional studies are needed to identify the molecule capable of transducing the electrical signal into Ca^{2+} discharge from IP_3-sensitive stores in adult sympathetic neurons.

It was demonstrated previously that insect dorsal unpaired median neurons possess a membrane voltage sensor that, independent of Ca^{2+} influx, causes G-protein activation, which subsequently leads to Ca^{2+} release from intracellular stores via phospholipase C and IP_3-receptor activation [6]. It remains to be determined whether the voltage-sensitive Ca^{2+} release mechanism in our study utilizes the same signaling pathway or whether the plasmalemmal voltage-sensor directly interacts with the IP_3 receptor in the ER membrane. The slow rise in cytosolic $[Ca^{2+}]$ during prolonged depolarizations in the absence of external Ca^{2+} suggests the involvement of intermediary steps in transducing the electrical signal into a Ca^{2+} release from intercellular stores. Moreover, dihydropyridine receptors have previously been reported to act as voltage sensors for a voltage-dependent, IP_3 receptor-mediated, slow Ca^{2+} signal in skeletal muscle cells [20]. A model was proposed in which the dihydropyridine receptor decodes the electrical signal into G-protein-dependent activation of phospholipase C to produce IP_3, which then diffuses to IP_3 receptors located on the ER and nuclear membrane, ultimately activating intracellular signaling cascades. Although our experiments provide no evidence for a role of dihydropyridine receptors as voltage-sensors in depolarization-evoked Ca^{2+} release in sympathetic ganglion neurons, our data suggests that both cell types share the signaling events downstream of their respective voltage-sensor.

Although 2-APB has been shown previously to inhibit IP_3-mediated Ca^{2+} release in neurons [31], it also exerts unspecific effects on Ca^{2+} entry in non-excitable cell types, e.g. via blockade of cation-selective channels encoded by the by transient receptor potential (TRP) genes [32]. However, our observation that xestospongin C at a concentration that has been shown previously to specifically inhibit IP_3 receptor signaling in a variety of mammalian cell types [33,34], similarly suppressed depolarization-induced increases in $[Ca^{2+}]_i$ in the absence of external Ca^{2+} support our conclusion that depolarization–evoked rises in $[Ca^{2+}]$ require functional IP_3 receptors.

Potential function of voltage-induced Ca^{2+} release in sympathetic neurons

Voltage-induced Ca^{2+} release constitutes a novel mechanism by which adult sympathetic ganglion neurons couple electrical activity to graded rises in intracellular $[Ca^{2+}]$. The extent to which this mechanism contributes to the increase in $[Ca^{2+}]$ that normally occurs in response to single or repetitive action potentials remains to be

quantitated. Eltit and co-workers previously demonstrated that tetanic stimulation of skeletal myotubes in the absence of extracellular Ca^{2+} gives rise to long-lasting, IP_3-generated, slow Ca^{2+} signals both in the nucleus and cytoplasm [34]. It will be interesting to determine whether repetitive electrical discharge of sympathetic ganglion neurons, such as occurring physiologically *in situ*, also results in slow Ca^{2+} signals similar to those evoked by high $[K^+]_e$ in the present study.

Although the magnitude of the depolarization-induced global Ca^{2+} transient is small compared to that of a transient elicited in normal $[Ca^{2+}]_e$, it is possible that Ca^{2+} is released into microdomains in which it may exert strong effects on exocytosis and/or Ca^{2+}-sensitive ion channels and enzymes, ultimately altering excitability, energy homeostasis, and transcriptional activity of the neuron. With regard to the latter, the elevations in nuclear fluo-4 fluorescence that were observed to occur concomitantly with those in the cytosol both in 2 and 0 mM $[Ca^{2+}]_i$, may play a role in transcriptional regulation [10]. The magnitude of depolarization-induced changes in nuclear fluo-4 fluorescence intensity in 2 mM $[Ca^{2+}]_e$ often reached saturation using gain settings that were optimized to monitor cytosolic fluorescence, precluding simultaneous measurements in both compartments.

Small elevations in cytosolic Ca^{2+} like those arising as a consequence depolarization-evoked IP_3-recpetor stimulation, may enhance the Ca^{2+} -sensitivity of nearby ryanodine receptors, thereby converting the cytoplasm in an excitable medium capable of producing regenerative Ca^{2+} responses.

Supporting Information

Go to:

S1 Fig

Effect of cadmium, a non-selective blocker of voltage-gated Ca^{2+} channels, on high $[K^+]_e$-induced cytosolic Ca^{2+} transients in postganglionic sympathetic neurons.

A and **B**: Family of current traces recorded from an isolated sympathetic neuron in the absence (A) and presence of 300 μM $CdCl_2$ in the external solution. Currents were evoked by 200-ms voltage steps, ranging from -70 to +50 mV in 10-mV increments. **C**: Peak *IBa*–voltage relationship for the cadmium-sensitive (circles) and–resistant (squares) currents shown in A and B. CdCl2 eliminated all inward currents.

(TIF)

Click here for additional data file. (485K, tif)

Funding Statement

Go to:

This work was supported by grants from the National Natural Science Foundation of China (81202509, http://www.nsfc.gov.cn/) to HS and the National Heart, Lung and Blood Institute (R01HL07165, http://www.nhlbi.nih.gov/) to MR. The funders had no role in study design, data collection and analysis, decision to publish, or preparation of the manuscript.

Data Availability

Go to:

All relevant data are within the paper and its Supporting Information files.

References

Go to:

1. Berridge MJ. Neuronal calcium signaling. Neuron. 1998; 21(1): 13–26. [PubMed]

2. Grienberger C, Konnerth A. Imaging calcium in neurons. Neuron. 2012; 73(5): 862–885. doi: 10.1016/j.neuron.2012.02.011 [PubMed]

3. Kim S, Yun HM, Baik JH, Chung KC, Nah SY, Rhim H. Functional interaction of neuronal Cav1.3 L-type calcium channel with ryanodine receptor type 2 in the rat hippocampus. J Biol Chem. 2007; 282(45): 32877–32889. [PubMed]

4. De Crescenzo V, Fogarty KE, Zhuge R, Tuft RA, Lifshitz LM, Carmichael J, et al. Dihydropyridine receptors and type 1 ryanodine receptors constitute the molecular machinery for voltage-induced Ca^{2+} release in nerve terminals. J Neurosci. 2006; 26(29): 7565–7574. [PubMed]

5. Ouardouz M, Nikolaeva MA, Coderre E, Zamponi GW, McRory JE, Trapp BD, et al. Depolarization-induced Ca^{2+} release in ischemic spinal cord white matter involves L-type Ca^{2+} channel activation of ryanodine receptors. Neuron. 2003; 40(1): 53–63. [PubMed]

6. Ryglewski S, Pflueger HJ, Duch C. Expanding the neuron's calcium signaling repertoire: intracellular calcium release via voltage-induced PLC and IP_3R activation. PLoS Biol. 2007; 5(4): e66 [PMC free article] [PubMed]

7. Kukwa W, Macioch T, Szulczyk PJ. Stellate neurones innervating the rat heart express N, L and P/Q calcium channels. J Auton Nerv Syst. 1998; 74(2–3): 143–151. [PubMed]

8. Namkung Y, Smith SM, Lee SB, Skrypnyk NV, Kim HL, Chin H, et al. Targeted disruption of the Ca^{2+} channel beta3 subunit reduces N- and L-type Ca^{2+} channel activity and alters the voltage-dependent activation of P/Q-type Ca^{2+} channels in neurons. Proc Natl Acad Sci U S A. 1998; 95(20): 12010–12015. [PMC free article] [PubMed]

9. Martínez-Pinna J, Lamas JA, Gallego R. Calcium current components in intact and dissociated adult mouse sympathetic neurons. Brain Res. 2002; 951(2): 227–236. [PubMed]

10. Wheeler DG, Barrett CF, Groth RD, Safa P, Tsien RW. CaMKII locally encodes L-type channel activity to signal to nuclear CREB in excitation-transcription coupling. J Cell Biol. 2008; 183(5): 849–863. doi: 10.1083/jcb.200805048 [PMC free article] [PubMed]

11. Akita T, Kuba K. Functional triads consisting of ryanodine receptors, Ca^{2+} channels, and Ca^{2+}-activated K^+ channels in bullfrog sympathetic neurons. Plastic modulation of action potential. J Gen Physiol. 2000; 116(5): 697–720. [PMC free article] [PubMed]

12. Albrecht MA, Colegrove SL, Hongpaisan J, Pivovarova NB, Andrews SB, Friel DD. Multiple modes of calcium-induced calcium release in sympathetic neurons I: attenuation of endoplasmic reticulum Ca^{2+} accumulation at low $[Ca^{2+}]_i$ during weak depolarization. J Gen Physiol. 2001; 118(1): 83–100. [PMC free article] [PubMed]

13. Li BY, Schild JH. Electrophysiological and pharmacological validation of vagal afferent fiber type of neurons enzymatically isolated from rat nodose ganglia. J Neurosci Methods. 2007; 164(1): 75–85. [PMC free article] [PubMed]

14. Friel DD, Tsien RW. A caffeine- and ryanodine-sensitive Ca^{2+} store in bullfrog sympathetic neurones modulates effects of Ca^{2+} entry on $[Ca^{2+}]_i$. J Physiol. 1992; 450: 217–246. [PMC free article] [PubMed]

15. Schoenmakers TJ, Visser GJ, Flik G, Theuvenet AP. CHELATOR: an improved method for computing metal ion concentrations in physiological solutions. Biotechniques. 1992; 12(6): 870–879. [PubMed]

16. Estève E, Eltit JM, Bannister RA, Liu K, Pessah IN, Beam KG, et al. A malignant hyperthermia-inducing mutation in RYR1 (R163C): alterations in Ca^{2+} entry, release, and retrograde signaling to the DHPR. J Gen

Physiol. 2010; 135(6): 619–628. doi: 10.1085/jgp.200910328 [PMC free article] [PubMed]

17. Satoh H, Delbridge LM, Blatter LA, Bers DM. Surface: volume relationship in cardiac myocytes studied with confocal microscopy and membrane capacitance measurements: species-dependence and developmental effects. Biophys J. 1996; 70(3): 1494–1504. [PMC free article] [PubMed]

18. Thayer SA, Hirning LD, Miller RJ. The role of caffeine-sensitive calcium stores in the regulation of the intracellular free calcium concentration in rat sympathetic neurons in vitro. Mol Pharmacol. 1988; 34(5): 664–673. [PubMed]

19. Beam KG, Bannister RA. Looking for answers to EC coupling's persistent questions. J Gen Physiol. 2010; 136(1): 7–12. doi: 10.1085/jgp.201010461 [PMC free article] [PubMed]

20. Araya R, Liberona JL, Cárdenas JC, Riveros N, Estrada M, Powell JA, et al. Dihydropyridine receptors as voltage sensors for a depolarization-evoked, IP_3R-mediated, slow calcium signal in skeletal muscle cells. J Gen Physiol. 2003; 121(1): 3–16. [PMC free article] [PubMed]

21. Nimmrich V, Gross G. P/Q-type calcium channel modulators. Br J Pharmacol. 2012; 167(4): 741–759. doi: 10.1111/j.1476-5381.2012.02069.x [PMC free article] [PubMed]

22. Bannister RA, Pessah IN, Beam KG. The skeletal L-type Ca^{2+} current is a major contributor to excitation-coupled Ca^{2+} entry. J Gen Physiol. 2009; 133(1): 79–91. doi: 10.1085/jgp.200810105 [PMC free article] [PubMed]

23. Hille B. Ion channels of excitable membranes. 3rd ed. Sunderland: Sinauer Associates, MA; 2001.

24. Belluzzi O, Sacchi O. Calcium currents in the normal adult rat sympathetic neurone. J Physiol. 1989; 412: 493–512. [PMC free article] [PubMed]

25. Usai C, Barberis A, Moccagatta L, Marchetti C. Pathways of cadmium influx in mammalian neurons. J Neurochem. 1999; 72(5): 2154–2161. [PubMed]

26. Hinkle PM, Shanshala ED 2nd, Nelson EJ. Measurement of intracellular cadmium with fluorescent dyes. Further evidence for the role of calcium channels in cadmium uptake. J Biol Chem. 1992; 267(35): 25553–25559. [PubMed]

27. Blumenstein Y, Maximyuk OP, Lozovaya N, Yatsenko NM, Kanevsky N, Krishtal O, et al. Intracellular Na^{+} inhibits voltage-dependent N-type Ca^{2+} channels by a G protein betagamma subunit-dependent mechanism. J Physiol. 2004; 556(Pt 1): 121–134. [PMC free article] [PubMed]

28. Polo-Parada L, Korn SJ. Block of N-type calcium channels in chick sensory neurons by external sodium. J Gen Physiol. 1997; 109(6): 693–702. [PMC free article] [PubMed]

29. Parri HR, Crunelli V. Sodium current in rat and cat thalamocortical neurons: role of a non-inactivating component in tonic and burst firing. J Neurosci. 1998; 18(3): 854–867. [PubMed]

30. Okamura Y, Murata Y, Iwasaki H. Voltage-sensing phosphatase: actions and potentials. J Physiol. 2009; 587(Pt 3): 513–520. doi: 10.1113/jphysiol.2008.163097 [PMC free article] [PubMed]

31. Bootman MD, Collins TJ, Mackenzie L, Roderick HL, Berridge MJ, Peppiatt CM. 2-aminoethoxydiphenyl borate (2-APB) is a reliable blocker of store-operated Ca^{2+} entry but an inconsistent inhibitor of $InsP_3$-induced Ca^{2+} release. FASEB J. 2002; 16(10): 1145–1150. [PubMed]

32. Xu SZ, Zeng F, Boulay G, Grimm C, Harteneck C, Beech DJ. Block of TRPC5 channels by 2-aminoethoxydiphenyl borate: a differential, extracellular and voltage-dependent effect. Br J Pharmacol. 2005;

145(4): 405–414. [PMC free article] [PubMed]

33. Bofill-Cardona E, Vartian N, Nanoff C, Freissmuth M, Boehm S. Two different signaling mechanisms involved in the excitation of rat sympathetic neurons by uridine nucleotides. Mol Pharmacol. 2000; 57(6): 1165–1172. [PubMed]

34. Eltit JM, Hidalgo J, Liberona JL, Jaimovich E. Slow calcium signals after tetanic electrical stimulation in skeletal myotubes. Biophys J. 2004; 86(5): 3042–3051. [PMC free article] [PubMed]